Published in final edited form as:

Microbiology (Reading). 2005 October ; 151(Pt 10): 3257–3265. doi:10.1099/mic.0.28095-0.

Allyl alcohol and garlic (*Allium sativum*) extract produce oxidative stress in *Candida albicans*

Katey M. Lemar[1], **Ourania Passa**[1], **Miguel A. Aon**[2], **Sonia Cortassa**[2], **Carsten T. Müller**[1], **Sue Plummer**[3], **Brian O'Rourke**[2], **David Lloyd**[1]

[1]Microbiology, Cardiff School of Biosciences, Main Building, Cardiff CF10 3TL, Wales, UK

[2]The Institute of Molecular Cardiobiology, Johns Hopkins Medicine, 720 Rutland Ave, 844 Ross Building, Baltimore, MD 21205-2195, USA

[3]Cultech Biospeciality Products Ltd, York Chambers, York Street, Swansea SA1 3NJ, Wales, UK

Abstract

Both the growth and respiration of *Candida albicans* are sensitive to extracts of *Allium sativum* and investigations into the anticandidal activities are now focussing on the purified constituents to determine the targets of inhibition. Of particular interest is allyl alcohol (AA), a metabolic product that accumulates after trituration of garlic cloves. Putative targets for AA were investigated by monitoring changes in intracellular responses after exposure of *C. albicans* cells to AA or a commercially available garlic extract. Two-photon laser scanning microscopy and other techniques were used. Changes typical of oxidative stress – NADH oxidation and glutathione depletion, and increased reactive oxygen species – were observed microscopically and by flow cytometry. Known targets for AA are alcohol dehydrogenases Adh1 and 2 (in the cytosol) and Adh3 (mitochondrial), although the significant decrease in NAD(P)H after addition of AA is indicative of another mechanism of action.

INTRODUCTION

Garlic (*Allium sativum*) has been used medicinally since before the time of the Sumerian civilization (2600–2100 BC), by when it was already widely cultivated in India and China (Harris *et al.*, 2001). Traditionally used as an antimicrobial agent, garlic has been reported also to modulate cardiovascular and immune functions as well as having antioxidant and anticancer properties. Garlic constituents were first investigated by Wertheim (1844); later studies showed that steam distillation gave diallyl disulphide, whereas more gentle extraction using ethanol at 25 °C or at subzero temperature released allicin and alliin respectively (Cavallito *et al.*, 1944). That the latter were examples of a number of cysteine sulphoxides and corresponding thiosulphinates was more recently demonstrated (Stoll & Seebeck, 1950, 1951; Lawson, 1996). Although the bioactive effects of garlic are attributed to the sulphur-containing molecules, other smaller metabolic breakdown products of these molecules have received increasing attention for their antimicrobial efficacy (Harris *et al.*, 2000; Banerjee *et al.*, 2003).

Correspondence, David Lloyd, LloydD@cf.ac.uk.

Allyl alcohol (AA), the focus of the present study, is produced from garlic in two ways: firstly by a self-condensation reaction of allicin and secondly by the reaction between alliin, the precursor of allicin, and water (Lawson, 1996). It is released after ingestion of garlic (Egen-Schwind *et al.*, 1992) and is present in exhaled air after ingestion of all garlic products, the highest concentration being after ingestion of freeze-dried garlic tablets (Laasko *et al.*, 1989). Mechanisms, first proposed by Block (1985), for the formation of AA in aqueous environments such as those found *in vivo* result from the transformation of the thiosulphinates such as diallyl trisulphide and diallyl disulphide (Block, 1985; Block *et al.*, 1992), with up to one-third of the 'lost' allyl groups during the transformation producing AA (Lawson, 1996). Recent investigations with rats reported that similar degradative metabolites are formed *in vivo* (Germain *et al.*, 2002).

Garlic as an antibacterial (Sharma *et al.*, 1977; Skyrme, 1997) has been the focus of detailed investigations recentzly on *Helicobacter pylori* (O'Gara *et al.*, 2000; Ross *et al.*, 2001). Differential inhibitory effects against *Escherichia coli* and *Lactobacillus casei*, whereby a 10-fold greater sensitivity was evident in the former (Rees *et al.*, 1993) have been studied in more detail with respect to the different membrane structures of Gram-positive and -negative bacteria (Cottrell, 2003). Antiprotozoal studies include those on *Entamoeba histolytica* (Mirelman *et al.*, 1987; Reuter, 1994) and *Giardia intestinalis* (Harris *et al.*, 2000); the anticandidal effects (Ghannoum, 1988, 1990; Lemar *et al.*, 2002, 2003) of garlic similarly include a wide range of ultrastructural lesions affecting cytoplasmic membranes, organelles and cytoskeletal organization. The widespread efficacy of this plant extract as an antimicrobial has been linked to the ease by which these molecules pass through cell membranes and react biologically at the low level of thiol bonds in amino acids (Miron *et al.*, 2000). That no example of acquired microbial resistance to garlic has been reported may also stem from its diverse modes of action and the multiplicity of intracellular targets that each bioactive component inactivates. Work with *G. intestinalis* (Harris *et al.*, 2000) and *Candida albicans* (Lemar *et al.*, 2002) has suggested that two of the simplest garlic constituents, diallyl disulphide and AA, are amongst the most potent; the former can be isolated by a process of steam distillation (Wertheim, 1844). More recent investigations, however, show that diallyl trisulphide is still more potent (Davis, 2005). A well-researched mechanism of AA toxicity is by its inhibition of alcohol dehydrogenase after its conversion to the toxic aldehyde acrolein (Rando, 1974). Acrolein (crotonaldehyde) and AA were the most toxic of 20 low-boiling-point compounds tested on the yeast *Candida utilis* (Sestakova *et al.*, 1976). More recent investigations have indicated that AA itself is not toxic to cells of the methylotrophic yeast *Pichia pastoris*, but it is toxic when oxidized via an alcohol oxidase pathway to acrolein (Johnson *et al.*, 1999). In rats, *in vivo*, AA is metabolized by liver alcohol dehydrogenase to acrolein (Mapoles *et al.*, 1994). Severe damage to the microtubules of rat hepatocyte mitochondria after exposure to AA (Vengerovskii *et al.*, 1989) was observed concomitantly with the depletion of glutathione (Nagelkerke *et al.*, 1991). However, more recent studies revealed that 100 μl AA per kg body weight in rats fed by gastric tube was not toxic to hepatocytes as determined by RNA extraction (Tygstrup *et al.*, 1997). These studies do not preclude this derivative from possible clinical use at the *in vivo* concentration required to be an effective antifungal. Effects of AA on *Saccharomyces cerevisiae* include disruption of cellular kinetics, redox balance and electrophoretic mobility

(Wills & Phelps, 1978). Acrolein is also known to deplete intracellular stores of glutathione and cause peroxidation of cellular lipids. This affects the permeability of the membrane and consequently undermines the viability of the cell (Glascott *et al.*, 1996).

In this study we investigated the biocidal mechanisms of AA on *C. albicans* by assessing its effects on cell physiology, and also on morphology using optical and electron imaging.

METHODS

Organism and culture

Candida albicans (Berkhout) 5134 was grown in YPD medium [Bacto-peptone 2% (w/v), Difco; yeast extract 1% (w/v), Oxoid; and glucose 2% (w/v)]. An early-stationary-phase culture was used as an inoculum (1:100 dilution in 50 ml) in 100 ml conical flasks. Growth was aerobic at 30 °C in a rotary shaker (150 r.p.m.). Cell numbers were determined with a haemocytometer slide (Fuschs-Rosenthal) after dilution in sterile medium. Optical density (OD_{450}) was measured using a Pye-Unicam SP-1400 spectrophotometer. Stock cultures of *C. albicans* were grown overnight at 30 °C and maintained at 4 °C on YPD agar containing 2% (w/v) agar (Oxoid), in the presence or absence of garlic preparation.

Garlic preparations

Garlic powder (provided by Cultech Biospeciality Products, Swansea, Wales, UK) was prepared to the required concentration in sterile growth medium. After 30 min the garlic powder extract (GPE) was centrifuged at 3900 *g* for 10 min and the supernatant passed through a sterile 0·2 μm filter (Millipore). Stock suspensions were prepared on the day of testing in PBS (pH 5·6) or appropriate media as stated. Concentration ranges for biocide assays for AA (0–10 mM) were prepared in sterile growth medium (AA was purchased from Sigma-Aldrich). MIC values were determined by the microtitre broth dilution method (Cottrell, 2003)

Ultrastructural investigations

Scanning electron microspcopy—Cells were fixed in 3 % (v/v) glutaraldehyde in PBS (pH 7·4) and dehydrated in increasing concentrations of ethanol (10%, v/v, increments, to 100 %). A drop was placed onto a round glass coverslip for critical-point drying (CPD 030; Balzers). The sample was mounted onto an aluminium slab (10 × 10 mm JEOL type; Agar Scientific) using silver paint (Agar Scientific). Sputter coating was performed in a sputter coater (S150B; Edwards) and the image viewed using a scanning electron microscope (5200LV; JEOL).

Transmission electron microscopy—Cells were fixed in cacodylate buffer, pH 6·9, containing 1 % (v/v) paraformaldehyde and 2 % (v/v) glutaraldehyde, at 4 °C for 1 h. The cells were centrifuged and dehydrated in successive washes of ethanol for 30 min. The pellet of cells was embedded in Spurr resin and ultrathin sections obtained (Ultratome III; LKB). The sections were mounted onto a 0.5 % Pioloform (in chloroform)-coated 3·05 mm copper grid then stained with 2% aqueous uranyl acetate and 2 % lead citrate before imaging on a transmission electron microscope (1210; JEOL).

Whole-cell respiration

Organisms in growth medium were harvested in exponential phase. Cells were washed and resuspended in 500 μl PBS pH 6·4. Measurement of glucose-supported O_2 consumption was performed at 30 °C in a thermostatically controlled closed electrode system (Rank) using a Teflon membrane electrode. Cell suspensions (40 μl) were injected into 2 ml PBS (pH 5·6) and continually stirred at 200 r.p.m.

Redox investigation: preincubation and conditions for microscopic examination

Early-stationary-phase cells were harvested and resuspended in PBS (pH 5·6). Samples (0·5 ml) were preloaded with 200 nM tetramethylrhodamine ethyl ester (TMRE) at 37 °C for 30 min before sample removal to the observation chamber and supplemented with 10 mM glucose. The dish containing the yeasts was equilibrated with unrestricted access to atmospheric oxygen on the stage of a Nikon E600FN upright microscope which was maintained at 30 °C. AA or GPE was subsequently added to the incubation mixture.

Fluorescent probes for two-photon laser scanning microscopy

The cationic potentiometric fluorescent dye TMRE was used to monitor changes in mitochondrial membrane potential, $\Delta\psi_m$. The large negative potential gradient across the inner mitochondrial membrane results in the accumulation of TMRE within the matrix compartment according to its Nernst potential (Loew *et al.*, 1993). Production of reactive oxygen species (ROS) was monitored with the ROS-sensitive fluorescent probe 5-(-6)-chloromethyl-2′,7′-dichlorohydrofluorescein diacetate (CM-H_2DCFDA, 10 μM). The acetate group of CM-H_2DCFDA is hydrolysed by esterases when it enters the cell and the molecule is trapped inside as the non-fluorescent 5-(-6)-chloromethyl-2′,7′-dichlorodihydrofluorescein (CM-H_2DCFH). CM-H_2DCFH was chosen because, unlike underivatized dichlorodihydrofluorescein, it is well retained in cells (Xie *et al.*, 1999) and, in this case, in the mitochondrial matrix (Aon *et al.*, 2003). Oxidation of CM-H_2DCFH by ROS, particularly by hydrogen peroxide (H_2O_2) and hydroxyl radical (Vanden Hoek *et al.*, 1997a, b), yields the fluorescent product carboxymethyldichlorofluorescein (CM-DCF), and indirectly measures mitochondrially produced O_2^- that has dismutated to H_2O_2 through the action of superoxide dismutase (Chance *et al.*, 1979; Turrens *et al.*, 1985).

Glutathione was monitored intracellularly by production of the fluorescent adduct glutathione-bimane (GSB) (Kosower & Kosower, 1987) as a result of the reaction of the cell permeant monochlorobimane (MCB, 50 μM) with reduced glutathione (GSH) catalysed by glutathione-*S*-transferase (GST) (Cortassa *et al.*, 2004). Reduced nicotinamide nucleotides were monitored by their autofluorescence under the imaging conditions optimized previously (Aon *et al.*, 2003).

Image acquisition and analysis

Images were recorded using a two-photon laser scanning microscope (Bio-Rad MRC-1024MP) with excitation at 740 nm (Tsunami Ti: Sapphire laser, Spectra-Physics) as described before (Aon *et al.*, 2003). Briefly, owing to the overlap in the cross-sections for two-photon excitation of the three fluorophores of interest (Xu *et al.*, 1996) (TMRE, CM-

DCF, and NADH or GSB) this wavelength permitted recording of $\Delta\psi_m$, ROS production, and NAD(P)H or GSH simultaneously. The red emission of TMRE was collected at 605 ± 25 nm; the green emission of CM-DCF was recorded at 525 ± 25 nm; and the blue emission of GSB detected at 480 ± 20 nm. NADH emission was collected as the total fluorescence <490 nm. At 3·5 s or 30 s intervals as indicated, 512 × 512 pixel 8-bit greyscale images of the three emission channels were collected simultaneously and stored.

While determining kinetics of GSB production in cells, about 10 images were recorded to get the cellular background of NADH before acute addition of 50 μM MCB. This was necessary because the NAD(P)H and GSB emissions were collected at similar wavelengths, i.e. 480–490 nm (Aon *et al.*, 2004; Cortassa *et al.*, 2004). At steady state, the NAD(P)H fluorescence levels (n = 14) represented 31 ± 1·2 % of the maximal GSB fluorescence levels attained (n=14), indicating an approximately threefold increase with respect to the background. Images were analysed offline using ImageJ software (Wayne Rasband, National Institutes of Health; http://rsb.info.nih.gov/ij/).

Fluorometric kinetic studies

The effect of AA and GPE on purified GST (from rabbit liver, Sigma cat. no. G8261, 6 U ml $^{-1}$ final concentration) as a function of GSH concentration was investigated. Increasing concentrations of GSH (in PBS pH 5·6) in the absence and presence of AA (0·5 or 1·0 mM) and GPE (5 or 10 mg ml^{-1}) were added to 3 ml PBS (pH 5·6); a subsequent addition of 50 μl GST was used to commence the reaction. Monochlorobimane (MCB, 2 μM final concentration; λ_{max} excitation 391 nm; λ_{max} emission 491 nm) was used as previously described (Aon *et al.*, 2003), and fluorescence measured using a Cary Eclipse fluorescence spectrophotometer (Varian).

Analysis of intracellular ROS using flow cytometry

Fluorescence distributions were obtained from 100 000 events per cell sample through a bandpass filter FL1 using a FACScalibur flow cytometer (BD Biosciences). Forward light scatter and side scatter were measured and used for gating the data collection. The fluorescence of gated cell populations was analysed using validated analysis software, WinMDI 2.8. Intracellular events in a population of *C. albicans* were analysed using CM-H_2DCFH as a marker for ROS as described previously (Aon *et al.*, 2003).

Materials

TMRE, CM-H_2DCFDA and MCB were purchased from Molecular Probes. All other reagents, including enzymes, were from Sigma-Aldrich unless specified.

RESULTS

Growth inhibition

Incubation with AA resulted in an extended lag phase and inhibition of growth during exponential phase (Fig. 1). Low concentrations of AA present throughout the experiment extended the time which the culture took to establish; increases in AA concentration resulted in decreases in growth rates – doubling times were as follows: control cultures (0 mM AA),

4 h; 0·25 mM AA (14·5 μg ml^{-1}), 8·3 h; 0·5 mM AA (29 μg ml^{-1}), 10·5 h. However, these AA-inhibited cultures eventually achieved the same maximum cell numbers as the controls (Fig. 1a). Doses of AA greater than 0·5 mM (29 μg ml^{-1}) resulted in complete inhibition (data not shown). Established cultures of *C. albicans* were able to tolerate higher concentrations of AA; when AA was added in mid-exponential phase, inhibition of growth was observed only at concentrations ⩾ 1 mM AA (29 μg ml^{-1}) (Fig. 1b). The IC_{50} (the concentration at which 50 % of the population is killed) for AA was 1 mM (58 μg ml^{-1}) at 10 h, and the MIC value was 0·1 mM (5·8 μg ml^{-1}). Colony growth on YPD medium indicated that AA is fungistatic at concentrations above 1 mM but fungicidal at concentrations above 2 mM (116 μg ml^{-1}).

Ultrastructural effects

Scanning electron microscopy—Aerobic growth of *C. albicans* cells in YPD medium at 30 °C gave typical yeast cells displaying the characteristic bud scars (Fig. 2ai). Development of pseudohyphae (chains of elongated unseparated blastospores) was only observed in cultures containing low concentrations of AA (Fig. 2aii). The external morphology of the cells after addition of 0·1 mM AA (5·8 μg ml^{-1}) (MIC) did not appear as smooth as that of untreated cells; this indicates a possible loss of cytosolic volume (Fig. 2aiii). Increasing the AA concentration further distorted the cell wall surface (Fig. 2aiv). Pseudohyphae were not observed at higher concentrations of AA. Neither untreated nor treated cultures produced true hyphae (presence of septa between elongated cells). Cells treated with GPE showed distortion of their outer surface, possibly due to loss of cytosolic volume; the collection of debris on the surface was also evident (Fig. 2b).

Transmission electron microscopy—Incubation of *C. albicans* in the presence of AA or GPE caused notable alterations in the internal morphology as compared to control cells (Fig. 3ai, bi). At high concentrations of AA (10 mM; 580 μg ml^{-1}) (Fig. 3aii), peripheral vacuoles were evident that were not visible in organisms from the control culture (Fig. 3ai). Treatment with GPE resulted in increased granulation of the cytoplasm and diminished cell membrane definition on increasing GPE concentration (Fig. 3bii, biii) in comparison with the control (Fig. 3bi).

Cellular respiration

Oxygen consumption rates increased as oxygen concentration decreased, down to about 50 % of air saturation value (Fig. 4). Successive additions of 5 mM AA (29 μg ml^{-1}) to the suspension of exponential-phase cells of *C. albicans* utilizing glucose supported respiration did not alter the rate of oxygen consumption. The final concentration was 20 mM AA (1·16 μg ml^{-1}), 200 times the MIC for AA. Successive additions of 120 μg GPE ml^{-1} (exponential-phase cells, glucose-supported respiration) had no effect up to a concentration of 2·4 mg ml^{-1}. Inhibition of respiration was observed at concentrations ⩾3·6 mg ml^{-1}. A final concentration of 4·8 mg GPE ml^{-1} caused 18 % reduction of the rate of oxygen consumption.

Confocal imaging of redox mechanisms

The key intracellular variables mitochondrial membrane potential ($\Delta\psi_m$), ROS and reduced glutathione (GSH) were monitored with fluorescent probes (TMRE, CM-DCF and MCB); the NAD(P)H redox status was imaged using autofluorescence (Fig. 5). A significant increase in $\Delta\psi_m$ was evident after treatment with 1 mM AA as compared to controls or exposure or 5 mg GPE ml^{-1} (Fig. 5i). A pattern of effects characteristic of oxidative stress was induced (i.e. high ROS, and a low level of GSH) was induced by addition of 1 mM AA (the IC_{50} value for this compound) to early-stationary-phase cells (Fig. 5). Addition of 5 mg GPE ml^{-1} caused a similar increase in ROS and depletion of GSH, but a decrease in NADH autofluorescence was also observed. A similar response was exhibited by exponential-phase cells (not shown). Low levels of ROS were localized in the mitochondria in control cells (Fig. 5aii); increased CM-DCF fluorescence was observed in both mitochondrial and cytoplasmic compartments after treatment with either GPE or AA (Fig. 5bii and 5cii). Autofluorescence of mitochondrial NAD(P)H was intense in control samples, but this signal was attenuated by oxidation after addition of GPE and AA (Fig. 5biii and 5ciii). Autofluorescence from mitochondrial and cytosolic NADH after AA addition was quantified as mean values of the pixel intensities. The decrease of NAD(P)H autofluorescence intensity for both cytosolic and mitochondrial compartments was significant after addition of AA ($P<0{\cdot}001$; $n=25$).

Formation of GSB, used to monitor glutathione levels before and after addition of challenge agents, indicated a general decrease in cell fluorescence (Fig. 5iv); AA gave the most significant decrease in GSB fluorescence (21 ± 0·7 a.u., $n=10$), to below the levels of the NAD(P)H autofluorescence control (55±0·9 a.u., $n=14$). The effect of GPE was less significant (Fig. 6).

Glutathione-*S*-transferase activity

That GST was not a target for AA or GPE was confirmed by fluorimetric analysis of the reaction of the purified enzyme. Inhibition of GST was not evident on increasing concentrations of either AA or GPE (results not shown). This suggests that GST is not one of the intracellular targets of AA or GPE.

Flow cytometric analysis

The fluorogenic compound CM-H_2DCFH is oxidized by ROS to give a fluorescent product (see Methods). Control suspensions of *C. albicans* loaded with this fluorogen showed only autofluorescence at 530 nm, whereas cells treated with AA and GPE fluoresced much more brightly. The fluorescence intensities increased as the concentration of either challenge agent was increased (Fig. 7).

DISCUSSION

These results further confirm that some garlic components possess significant anticandidal properties (Lemar *et al.*, 2002) and that AA, a metabolic breakdown product of allicin, plays a major role in the inhibition of growth of *C. albicans*.

Allicin is considered one of the principal antimicrobial constituents of triturated garlic cloves (Cavallito *et al.*, 1944), and although it has microbicidal activity *in vitro* (Ankri & Mirelman, 1999), its half-life in tissues is too short to ensure appreciable pathogen damage (Koch, 1996). Systemic levels of the metabolic products of allicin are reported to be relatively high (Egen-Schwind *et al.*, 1992), and researchers have now turned their interest to these constituents as possessing considerable antimicrobial properties. AA is found in exhaled air after ingestion of freeze-dried garlic tablets (Laasko *et al.*, 1989). As it is a known hepato-toxicant, its use in pure form would have to be administered carefully; however, dosage up to 100 μl AA per kg body weight in rats after administration by gastric tube presented no toxicity to hepatocytes (Tygstrup *et al.*, 1997). These studies do not preclude the use of this constituent for clinical administration at the *in vivo* concentration required to produce an antifungal effect. Conversion of AA to acrolein can lead to subsequent inhibition of alcohol dehydrogenases (Rando, 1974). *S. cerevisiae* has 20 alcohol dehydrogenases (Kruckerberg & Dickinson, 2004), but the best understood and possibly the most important enzyme targets involved in AA toxicity are the cytosolically located Adh1 and 2, involved in ethanol formation and growth on ethanol respectively, and Adh3, which is mitochondrial. The functions of Adh3 are not entirely understood, but it has been postulated to be involved in a redox shuttle, transferring mitochondrial NADH to the cytosol (Bakker *et al.*, 2000). Improvements in methods for measuring mitochondrial redox state (see Chance, 2004, for a review) have allowed us to detect a decrease in both cytosolic and mitochondrial NADH. Results suggest that although it is possible that all three of these enzymes are targeted by AA, another site of action is involved to produce this effect (Fig. 5ciii). Depletion of NAD(P)H, the co-substrate for glutathione reductase, would diminish the recovery of the GSH pools in both compartments. As AA depletes glutathione (Glascott *et al.*, 1996), one might predict an increase in ROS. Confocal imaging and quantitative analysis does indeed indicate the depletion of glutathione and increase in ROS when cells are treated with AA (Figs 5, 6 and 7). Electron microscopy of cells treated with AA also indicates that mitochondria may be a target for AA (Fig. 3). However, decreased respiration, as observed with GPE and other garlic constituents (K. M. Lemar and others, unpublished), was not observed for AA. This may be explained by the fact that the alcohol dehydrogenase function is not implicated in glucose respiration, as when organisms are grown in the presence of excess glucose, alcohol dehydrogenase is inactivated (Gonzalez *et al.*, 2000). The conversion of AA to the toxic aldehyde acrolein would therefore not occur. Exposure to AA may thus impair *C. albicans* viability through mechanisms not directly associated with mitochondrial function.

The enzyme GST, associated with maintaining redox balance, is a target of a different garlic constituent, diallyl disulphide (DADS) (K. M. Lemar and others, unpublished). Our experiments demonstrated that it is not a target for AA. This is perhaps unsurprising, as the two compounds have quite different structures. However, this observation assists in our understanding of why GPE has such a broad spectrum of activity. The multiple metabolic constituents produced by the plant (many of which remain to be explored), may have many different targets, and hence produce diverse effects on cell processes. Its extensive repertoire of inhibitory constituents makes garlic an interesting potential alternative to single-site-specific antibiotics or synthetic organic compounds for combating *C. albicans* infections.

However, the presence of toxic metabolites, such as AA itself, may limit the dose that can be administered. Previous investigations concerning the antifungal properties of whole garlic extracts compared to some of its breakdown products have shown that they have similar MICs, with similar mechanisms of action, such as glutathione depletion and reaction with thiol groups (Davis *et al.*, 2003). AA may well be an exception due to the activity of the acrolein/alcohol dehydrogenase pathway activity; however its antifungal efficacy *in vitro* would have to be determined by MIC studies.

Abbreviations

$\Delta\psi_m$	mitochondrial membrane potential
AA	allyl alcohol
CM-DCF	carboxymethyldichlorofluorescein
CM-H_2DCFDA	5-(-6)-chloromethyl-2′,7′-dichlorohydrofluorescein diacetate
CM-H_2DCFH	5-(-6)-chloromethyl-2′,7′-dichlorodihydrofluorescein
GPE	garlic powder extract
GSB	glutathione-bimane
GST	glutathione-*S*-transferase
MCB	monochlorobimane
ROS	reactive oxygen species
TMRE	tetramethylrhodamine ethyl ester

REFERENCES

Ankri S, Mirelman D. Antimicrobial properties of allicin from garlic. Microbes Infect. 1999; 1:125–129. [PubMed: 10594976]

Aon MA, Cortassa S, Marban E, O'Rourke B. Synchronized whole cell oscillations in mitochondrial metabolism triggered by a local release of reactive oxygen species in cardiac myocytes. J Biol Chem. 2003; 278:44735–44744. [PubMed: 12930841]

Aon MA, Cortassa S, O'Rourke B. Percolation and criticality in a mitochondrial network. Proc Natl Acad Sci U S A. 2004; 101:4447–4452. [PubMed: 15070738]

Bakker BM, Bro C, Kotter P, Luttik MA, van Dijken JP, Pronk JT. The mitochondrial alcohol dehydrogenase Adh3p is involved in a redox shuttle in *Saccharomyces cerevisiae*. J Bacteriol. 2000; 182:4730–4737. [PubMed: 10940011]

Banerjee SK, Mukherjee PK, Maulik SK. Garlic as an antioxidant: the good, the bad and the ugly. Phytother Res. 2003; 17:97–106. [PubMed: 12601669]

Block E. The chemistry of garlic and onions. Sci Am. 1985; 252:114–119. [PubMed: 3975593]

Block E, Putnam D, Zhao SH. *Allium* chemistry: GC-MS analysis of thiosulfinates and related compounds from onion, leek, scallion, shallot, chive, and Chinese chive. J Agric Food Chem. 1992; 40:2431–2438.

Cavallito C, Bailey JH, Buck JS. Allicin, the antibacterial principle of *Allium sativum* II. Its precursor and "essential oil" of garlic. J Am Chem Soc. 1944; 67:1032–1033.

Chance B. Mitochondrial NADH redox state, monitoring discovery and deployment in tissue. Methods Enzymol. 2004; 385:361–370. [PubMed: 15130749]

Chance B, Sies H, Boveris A. Hydroperoxide metabolism in mammalian organs. Physiol Rev. 1979; 59:527–605. [PubMed: 37532]

Cortassa S, Aon MA, Winslow RL, O'Rourke B. A mitochondrial oscillator dependent on reactive oxygen species. Biophys J. 2004; 87:2060–2073. [PubMed: 15345581]

Cottrell, S. PhD thesis. Cardiff School of Biosciences, Cardiff University; 2003. An investigation into the antibacterial effects of Allium sativum (garlic).

Davis SR. An overview of the antifungal properties of allicin and its breakdown products - the possibility of a safe and effective antifungal prophylactic. Mycoses. 2005; 48:95–100. [PubMed: 15743425]

Davis SR, Perrie R, Apitz-Castro R. The in vitro susceptibility of *Scedosporium prolificans* to ajoene, allitridium and a raw extract of garlic (*Allium sativum*). J Antimicrob Chemother. 2003; 51:593–597. [PubMed: 12615859]

Egen-Schwind C, Eckard R, Jekat FW, Winterhoff H. Pharmacokinetics of vinyldithiins, transformation products of allicin. Planta Med. 1992; 58:8–13. [PubMed: 1620748]

Germain E, Auger J, Ginies C, Siess MH, Teyssier C. *In vivo* metabolism of diallyl disulphide in the rat: identification of two new metabolites. Xenobiotica. 2002; 32:1127–1138. [PubMed: 12593760]

Ghannoum MA. Studies on the anticandidal mode of action of *Allium sativum* (garlic). J Gen Microbiol. 1988; 134:2917–2924. [PubMed: 3076177]

Ghannoum MA. Inhibition of Candida adhesion to buccal epithelial cells by an aqueous extract of *Allium sativum* (garlic). J Appl Bacteriol. 1990; 68:163–169. [PubMed: 2318745]

Glascott PA Jr, Gilfor E, Serroni A, Farber JL. Independent antioxidant action of vitamins E and C in cultured rat hepatocytes intoxicated with allyl alcohol. Biochem Pharmacol. 1996; 52:1245–1252. [PubMed: 8937432]

Gonzalez E, Fernandez MR, Larroy C, Sola L, Pericas MA, Pares X, Biosca JA. Characterization of a (2*R*,3*R*)-2,3-butanediol dehydrogenase as the *Saccharomyces cerevisiae* YAL060W gene product. Disruption and induction of the gene. J Biol Chem. 2000; 275:35876–35885. [PubMed: 10938079]

Harris JC, Plummer S, Turner MP, Lloyd D. The microaerophilic flagellate *Giardia intestinalis: Allium sativum* (garlic) is an effective antigiardial. Microbiology. 2000; 146:3119–3127. [PubMed: 11101670]

Harris JC, Cotrell SL, Plummer S, Lloyd D. Antimicrobial properties of *Allium sativum* (garlic). Appl Microbiol Biotechnol. 2001; 57:282–286. [PubMed: 11759674]

Johnson MA, Waterham HR, Ksheminska GP. Positive selection of novel peroxisome biogenesis-defective mutants of the yeast *Pichia pastoris*. Genetics. 1999; 151:1379–1391. [PubMed: 10101164]

Koch, H. Biopharmaceutics of garlic's effective compounds. In: Koch, HP, Lawson, LD, editors. Garlic: the Science and Therapeutic Application of Allium sativum L and related species. Baltimore: Williams & Wilkins; 1996. 213–220.

Kosower NS, Kosower EM. Thiol labeling with bromobimanes. Methods Enzymol. 1987; 143:76–84. [PubMed: 3657564]

Kruckerberg, AL, Dickinson, JR. Carbon metabolism. In: Schweizer, JRDM, editor. Metabolism and Molecular Physiology of Saccharomyces cerevisiae. Boca Raton, FL: CRC Press; 2004.

Laasko I, Seppanen-Laasko T, Hiltunen R, Muller B, Jansen H, Knoblock K. Volatile garlic odour components: gas phases and absorbed exhaled air analysed by headspace gas chromatography-mass spectrometry. Planta Med. 1989; 55:257–261. [PubMed: 17262412]

Lawson, LD. The composition and chemistry of garlic cloves and processed garlic. In: Koch, HP, Lawson, LD, editors. Garlic: The Science and Therapeutic Application of Allium sativum and Related Species. Baltimore: Williams & Wilkins; 1996. 37–107.

Lemar KM, Turner MP, Lloyd D. Garlic (*Allium sativum*) as an anti-Candida agent: a comparison of the efficacy of fresh garlic and freeze-dried extracts. J Appl Microbiol. 2002; 93:398–405. [PubMed: 12174037]

Lemar KM, Muller CT, Plummer S, Lloyd D. Cell death mechanisms in the human opportunistic pathogen *Candida albicans*. J Eukaryot Microbiol. 2003; 50(Suppl):685–686. [PubMed: 14736219]

Loew LM, Tuft RA, Carrington W, Fay FS. Imaging in five dimensions: time-dependent membrane potentials in individual mitochondria. Biophys J. 1993; 65:2396–2407. [PubMed: 8312478]

Mapoles JE, Iwahashi M, Lucas D, Zimmerman BT, Simon FR. Acetaldehyde exposure causes growth inhibition in a Chinese hamster ovary cell line that expresses alcohol dehydrogenase. Alcohol Clin Exp Res. 1994; 18:632–639. [PubMed: 7943667]

Mirelman D, Monheit D, Varon S. Inhibition of growth of *Entamoeba histolytica* by allicin, the active principle of garlic extract (*Allium sativum*). J Infect Dis. 1987; 156:243–244. [PubMed: 2885381]

Miron T, Rabinkov A, Mirelman D, Wilchek M, Weiner L. The mode of action of allicin: its ready permeability through phospholipid membranes may contribute to its biological activity. Biochim Biophys Acta. 2000; 1463:20–30. [PubMed: 10631291]

Nagelkerke JF, van de Water B, Twiss IM, Zoetewey JP, de Bont HJ, Dogterom P, Mulder GJ. Role of microtubuli in secretion of very-low-density lipoprotein in isolated rat hepatocytes: early effects of thiol reagents. Hepatology. 1991; 14:1259–1268. [PubMed: 1959877]

O'Gara EA, Hill DJ, Maslin DJ. Activities of garlic oil, garlic powder, and their diallyl constituents against *Helicobacter pylori*. Appl Environ Microbiol. 2000; 66:2269–2273. [PubMed: 10788416]

Rando RR. Allyl alcohol-induced irreversible inhibition of yeast alcohol dehydrogenase. Biochem Pharmacol. 1974; 23:2328–2331. [PubMed: 4368394]

Rees L, Minney SF, Plummer NT, Slater JH, Skyrme DA. A quantitative assessment of the anti-microbial activity of garlic (*Allium sativum*). World J Microbiol Biotechnol. 1993; 9:303–307. [PubMed: 24420031]

Reuter R. *Allium sativum* and *Allium ursinium*: part 2-pharmacology and medical application. Phytomedicine. 1994; 2:73–91.

Ross ZM, O'Gara EA, Hill DJ, Sleightholme HV, Maslin DJ. Antimicrobial properties of garlic oil against human enteric bacteria: evaluation of methodologies and comparisons with garlic oil sulfides and garlic powder. Appl Environ Microbiol. 2001; 67:475–480. [PubMed: 11133485]

Sestakova M, Adamek L, Stros F. Effect of crotonaldehyde on the metabolism of *Candida utilis* during the production of single cell protein from ethanol. Folia Microbiol. 1976; 21:444–454. [PubMed: 1033115]

Sharma VD, Sethi MS, Kumar A, Rarotra JR. Antibacterial property of *Allium sativum* Linn. in vivo and in vitro studies. Indian J Exp Biol. 1977; 15:466–468. [PubMed: 598878]

Skyrme, D. PhD thesis. University of Wales, College of Cardiff; 1997. An investigation into the anti-microbial activity of Allium sativum.

Stoll A, Seebeck E. Synthesis of natural alliin. Experientia. 1950; 6:330.

Stoll A, Seebeck E. The specificity of the alliinase from *Allium sativum*. C R Hebd Seances Acad Sci. 1951; 232:1441–1442.

Turrens JF, Alexandre A, Lehninger AL. Ubisemiquinone is the electron donor for superoxide formation by complex III of heart mitochondria. Arch Biochem Biophys. 1985; 237:408–414. [PubMed: 2983613]

Tygstrup N, Jensen SA, Krog B, Dalhoff K. Expression of liver functions following sub-lethal and non-lethal doses of allyl alcohol and acetaminophen in the rat. J Hepatol. 1997; 27:156–162. [PubMed: 9252090]

Vanden Hoek TL, Li C, Shao Z, Schumacker PT, Becker LB. Significant levels of oxidants are generated by isolated cardiomyocytes during ischemia prior to reperfusion. J Mol Cell Cardiol. 1997a; 29:2571–2583. [PubMed: 9299379]

Vanden Hoek TL, Shao Z, Li C, Schumacker PT, Becker LB. Mitochondrial electron transport can become a significant source of oxidative injury in cardiomyocytes. J Mol Cell Cardiol. 1997b; 29:2441–2450. [PubMed: 9299367]

Vengerovskii AI, Sedykh IM, Saratikov AS. Effectiveness of hepatoprotective agents in experimental allyl alcohol poisoning. Gig Tr Prof Zabol. 1989:46–47.

Wertheim, T. Protozoology. London: Bailliére, Tindall & Cassel; 1844.

Wills C, Phelps J. Functional mutants of yeast alcohol dehydrogenase affecting kinetics, cellular redox balance, and electrophoretic mobility. Biochem Genet. 1978; 16:415–432. [PubMed: 367361]

Xie Z, Kometiani P, Liu J, Li J, Shapiro JI, Askari A. Intracellular reactive oxygen species mediate the linkage of Na^+/K^+-ATPase to hypertrophy and its marker genes in cardiac myocytes. J Biol Chem. 1999; 274:19323–19328. [PubMed: 10383443]

Xu C, Zipfel W, Shear JB, Williams RM, Webb WW. Multiphoton fluorescence excitation: new spectral windows for biological nonlinear microscopy. Proc Natl Acad Sci U S A. 1996; 93:10763–10768. [PubMed: 8855254]

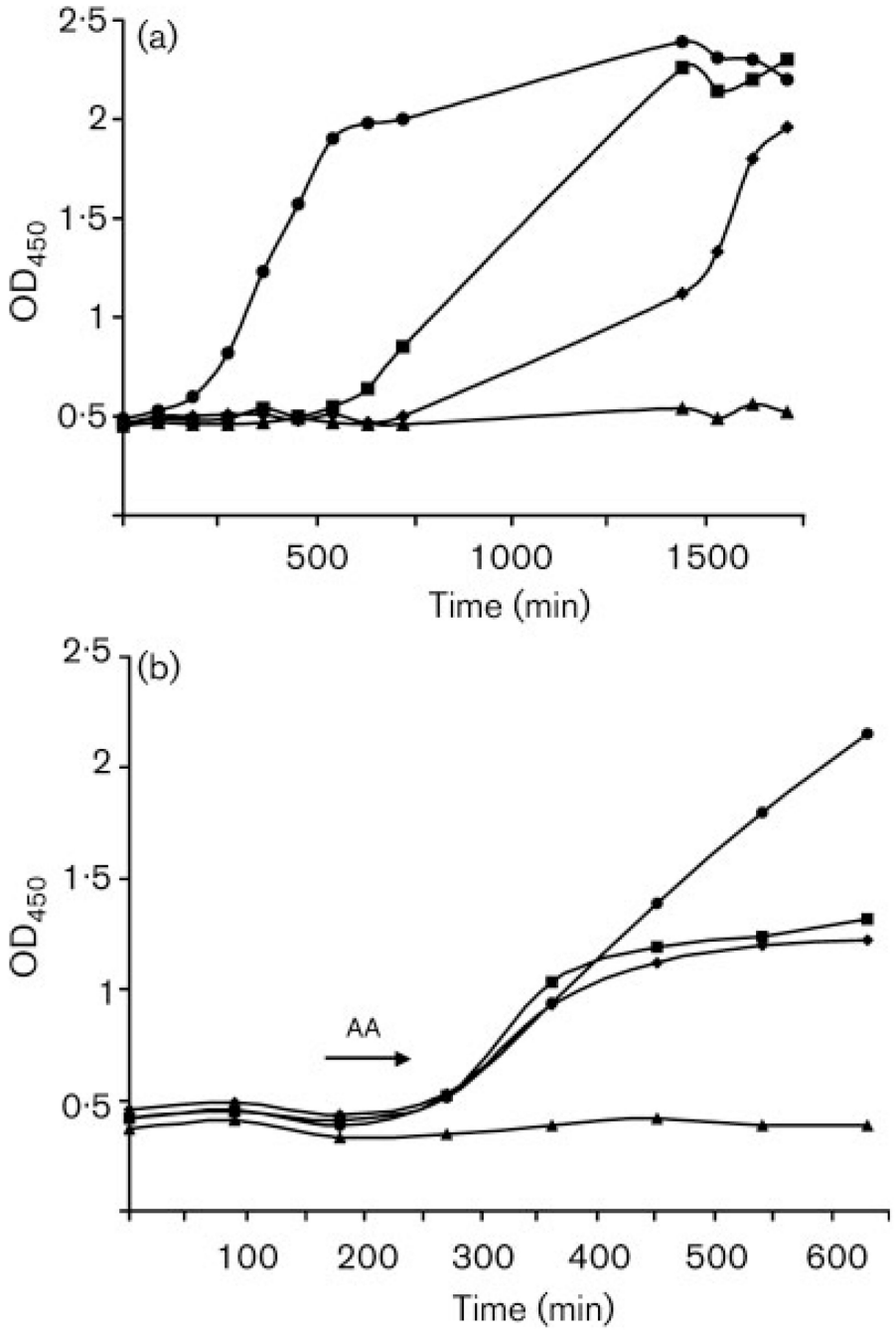

Fig. 1.

Effect of AA on growth of *C. albicans* after addition at early stationary phase and mid-exponential phase. (a) Early stationary phase: ●, 0 mM; ■, 0·25 mM (14·5 μg ml^{-1}); ◆ 0·5 mM (29 μg ml^{-1}); ▲, uninoculated control. (b) Mid-exponential phase (as indicated by arrow): ●, 0 mM; ■, 1·0 mM (58 μg ml^{-1}); ◆, 1·5 mM (87 μg ml^{-1}); ▲, uninoculated control. Results are representative of triplicate experiments. The discrepancies in the time scales between the panels is due to extension of the lag phase on exposure to AA.

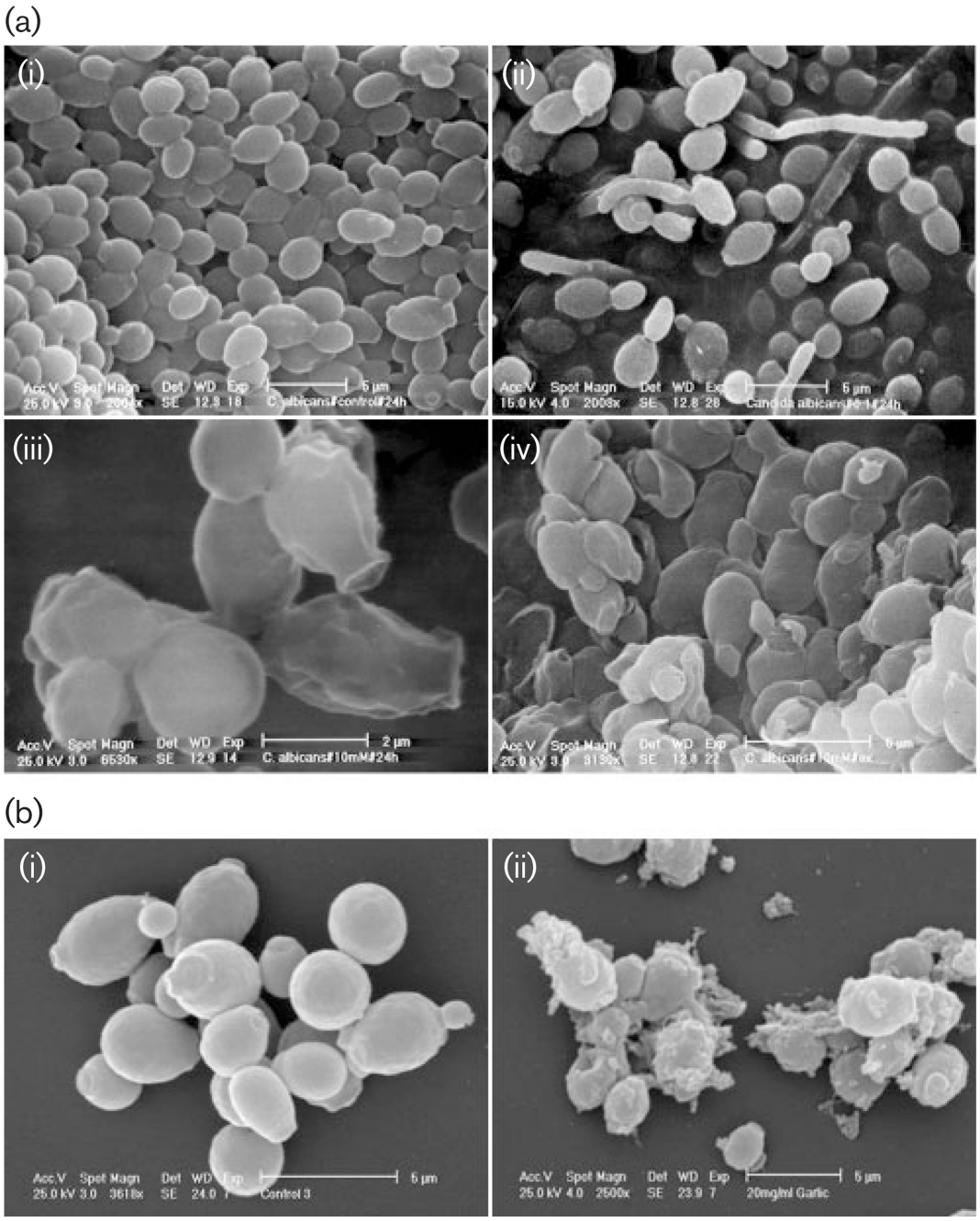

Fig. 2.

Scanning electron micrographs of *C. albicans* treated with AA or GPE (a) AA: (i) untreated culture, (ii) 0·1 mM AA (5·8 mg ml^{-1}), (iii) 1·0 mM (58 μg ml^{-1}) AA, (iv) 10 mM (580 μg ml^{-1}; high concentration used to induce extreme effects). (b) GPE (i) untreated control, (ii) 20 mg GPE ml^{-1}.

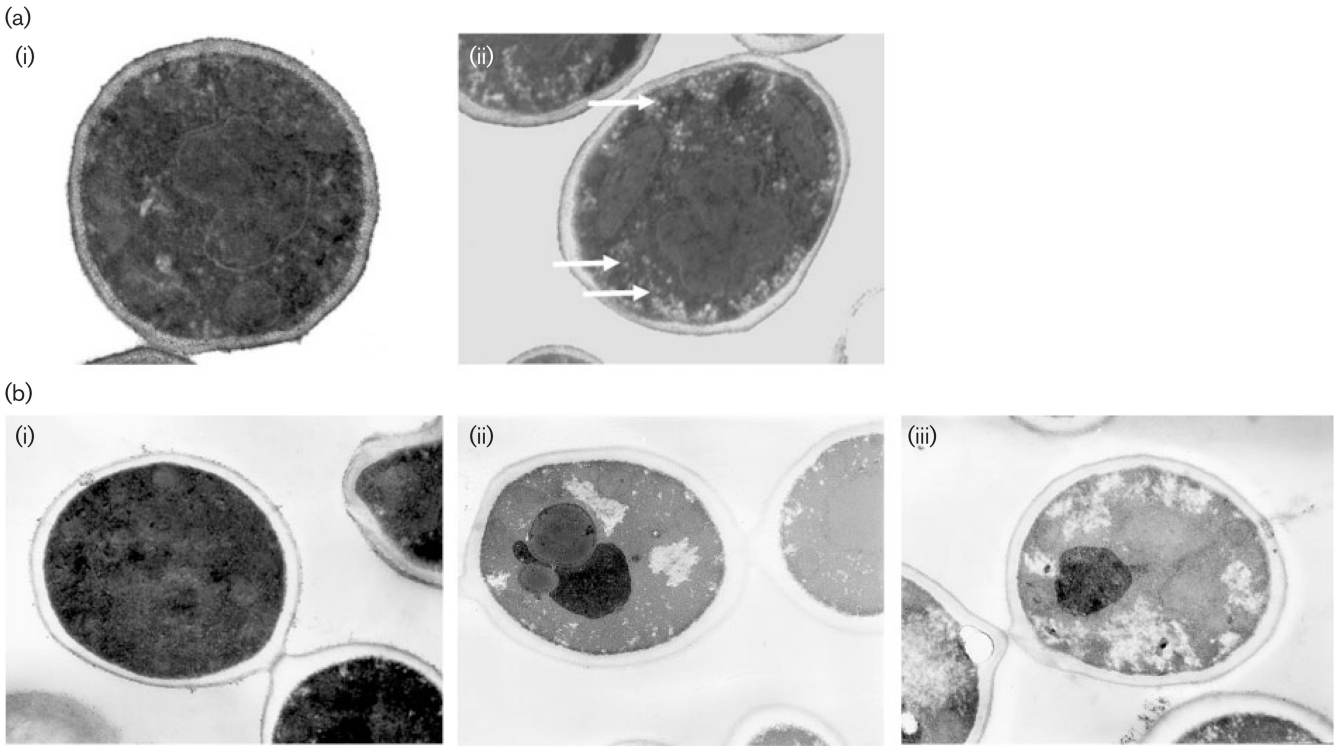

Fig. 3.

Transmission electron micrographs of *C. albicans* treated with AA or GPE. (a) AA: (i) untreated control, (ii) 10 mM AA; note increased granulation of cytosol and appearance of peripheral vacuoles (white arrows) in the presence of AA. (b) GPE: (i) untreated control, (ii) 1 mg GPE ml^{-1}, (iii) 30 mg GPE ml^{-1}; pictures taken at magnification of × 18000.

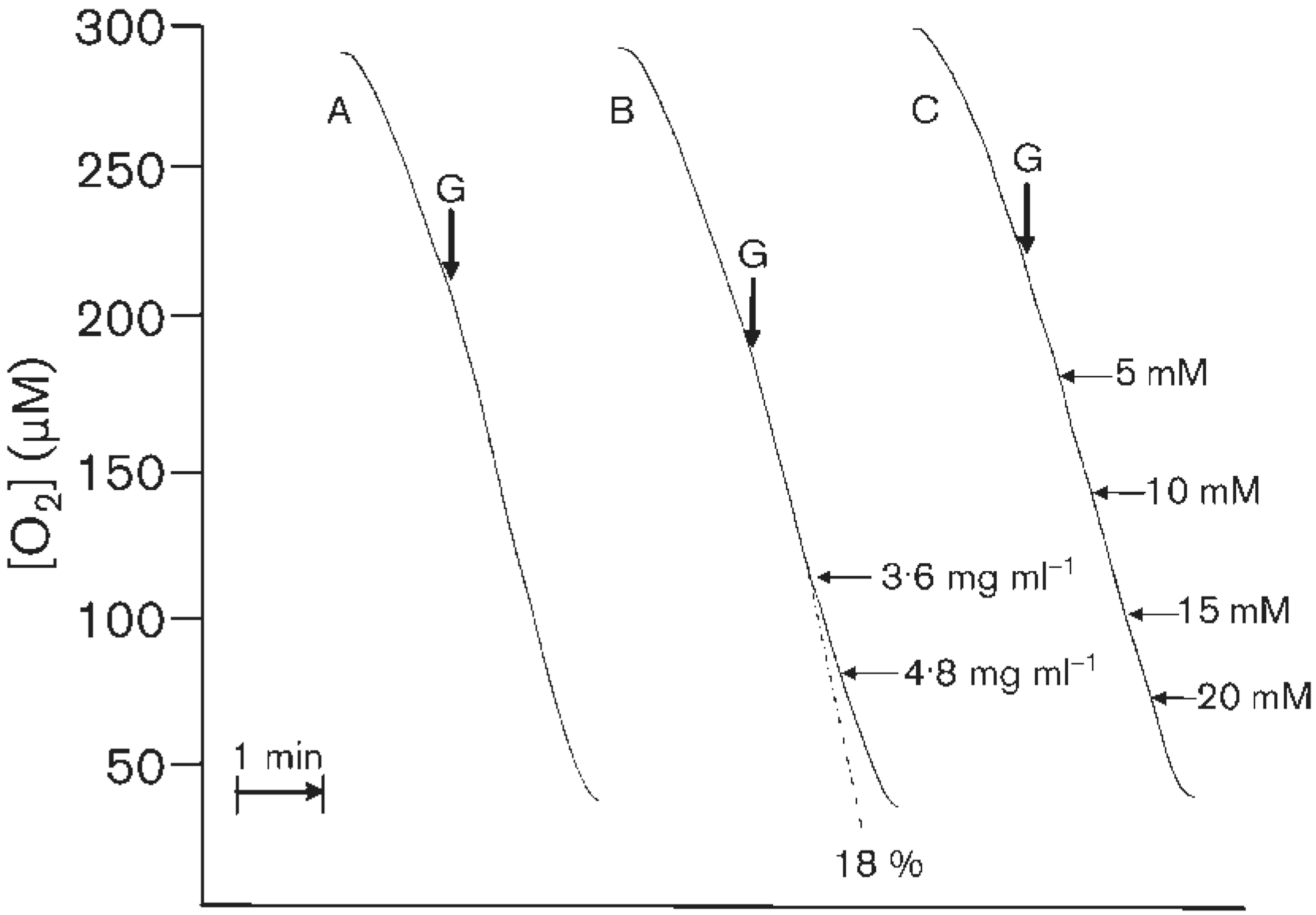

Fig. 4.

Oxygen consumption of organisms harvested from an exponentially growing culture of *C. albicans*. Endogenous rates (addition of 100 mM glucose indicated by arrows 'G') are shown for control (A), garlic powder extract (B) and AA (C). Horizontal arrows indicate additions of GPE or AA; adjacent numbers indicate concentration. Percentage inhibition at a final concentration of 4·8 mg GPE ml^{-1} is indicated below trace B. The dotted line indicates rate of oxygen consumption if no inhibition had occurred. Cell density was 8×10^6 cells ml^{-1}. Traces are typical of results with three batches of cells.

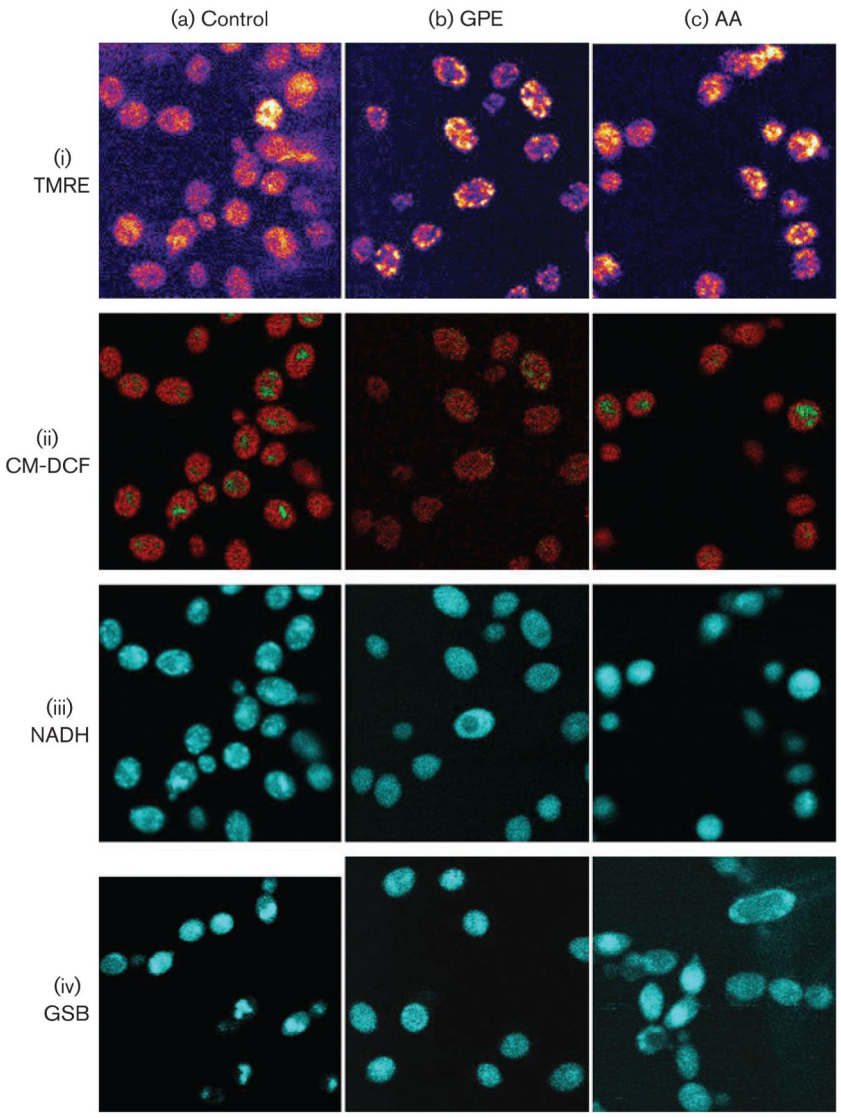

Fig. 5.

Fluorescent monitoring by two-photon scanning laser microscopy of *C. albicans* control and treated cells (1 mM AA or 5 mg GPE ml^{-1}): (i) mitochondrial membrane potential, monitored with TMRE; (ii) ROS, monitored with CM-DCF; (iii) NAD(P)H, monitored by autofluorescence; (iv) GSH, monitored by fluorescence of GSB produced from added MCB. Images of stationary-phase cells were obtained as described in Methods. Laser conditions were as follows. (i) Untreated cells, 5 × accumulated image, 80% laser intensity; 1 mM AA, no accumulation, 40 % laser intensity; 5 mg GPE ml^{-1}, 3 × accumulated image, 40% laser intensity. (ii, iii, iv) Untreated, 1 mM AA and 5 mg ml^{-1} GPE all 3 × accumulated image, 40% laser intensity.

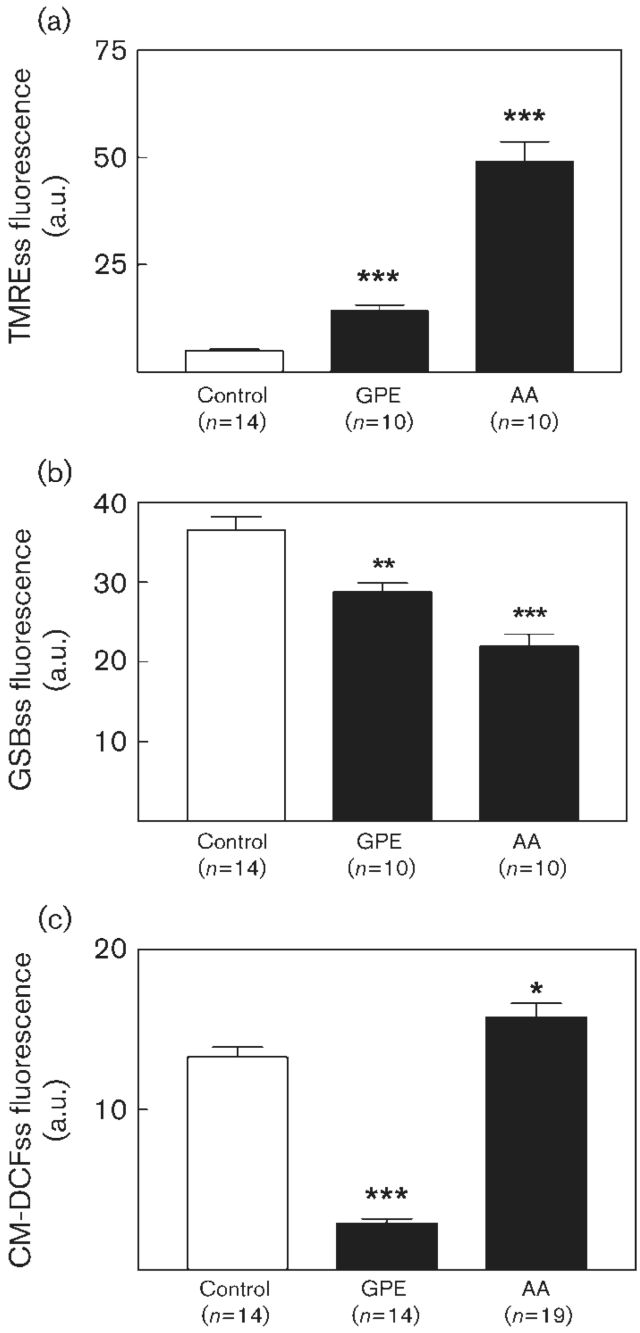

Fig. 6.

Effects of garlic components on fluorescence signals from two-photon microscopy images. *C. albicans* cells were harvested in early stationary phase and exposed to different garlic components at room temperature. The steady-state (ss) levels of fluorescence (as the mean pixel intensity of a normal distribution, in arbitrary units) from TMRE, GSB and CM-DCF probes after 30 min treatment with 1 mM AA or 5 mg GPE ml^{-1} were determined. Asterisks indicate the level of significance: ***, $P<0{\cdot}001$; **, $P<0{\cdot}01$; *, $P<0{\cdot}05$ versus control.

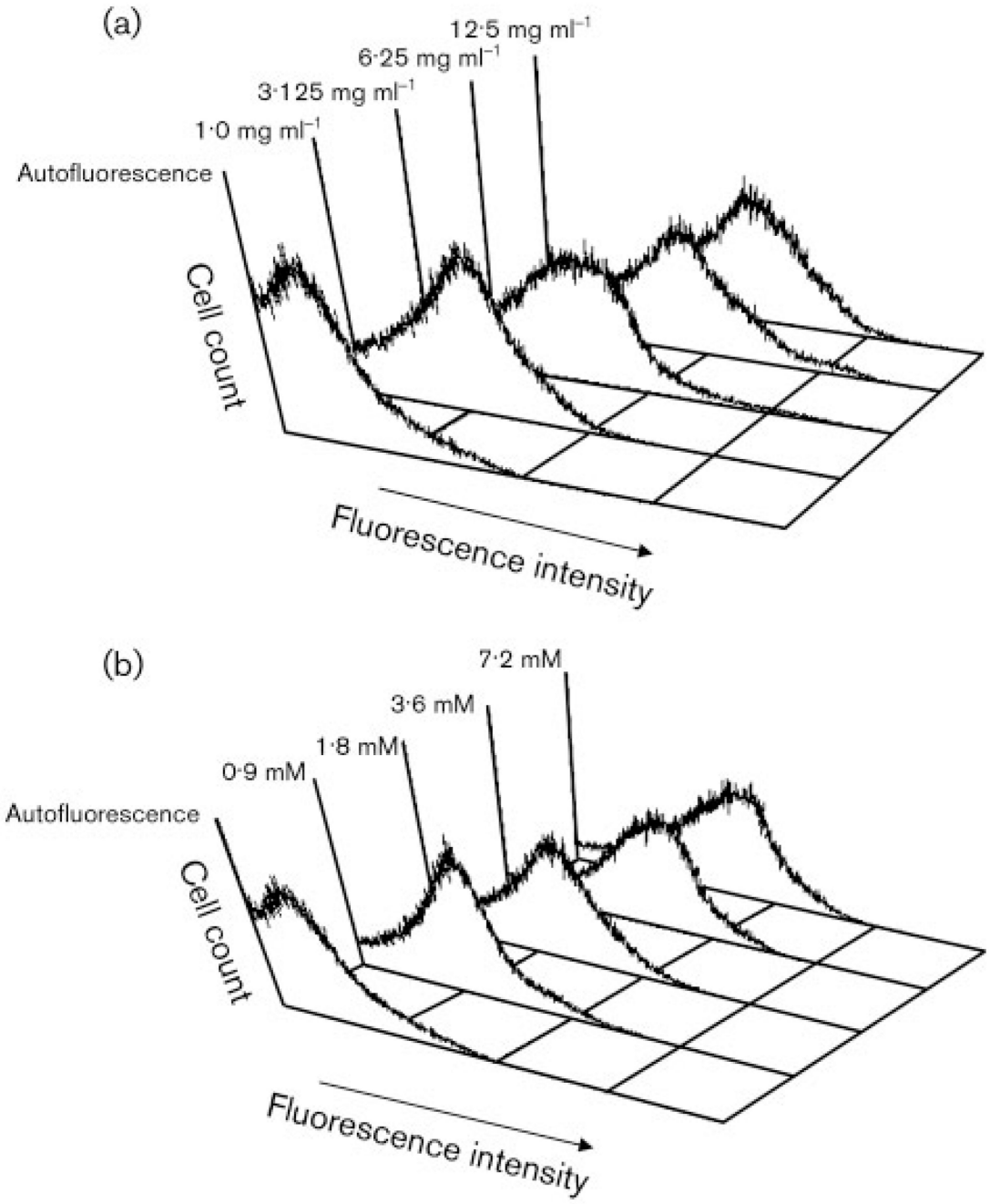

Fig. 7.
Fluorescence of *C. albicans* cells treated with (a) GPE or (b) AA at the concentrations indicated.